

## Electronic supplementary information

### MgFePO<sub>4</sub>F as a feasible cathode material for magnesium batteries

Zhen-Dong Huang<sup>a,\*</sup>, Titus Masese<sup>a</sup>, Yuki Oriksa<sup>a</sup>, Takuya Mori<sup>a</sup>, Taketoshi Minato<sup>b</sup>,

Cedric Tassel<sup>c</sup>, Yoji Kobayashi<sup>c</sup>, Hiroshi Kageyama<sup>c</sup>, Yoshiharu Uchimoto<sup>a</sup>

<sup>a</sup> Graduate School of Human and Environmental Studies, Kyoto University, Yoshida-nihonmatsu-Cho, Sakyo-ku, Kyoto 606-8501, Japan

<sup>b</sup> Office of Society-Academia Collaboration for Innovation, Kyoto University, Gokasho, Uji 611-0011, Japan

<sup>c</sup> Graduate School of Engineering, Kyoto University, Katsura-chu, Nishikyo-ku, Kyoto 615-8510, Japan

#### Experimental

##### Material Synthesis

Stoichiometric MgFePO<sub>4</sub>F (MFPF) powders were prepared via the conventional solid-state carbothemal method. MFPF was obtained starting from a rigorous mixing of stoichiometric quantities of MgHPO<sub>4</sub> (received from Sigma), FeC<sub>2</sub>O<sub>4</sub> · 2H<sub>2</sub>O (2N — Junsei Chemical) and NH<sub>4</sub>F (received from Wako) powders which were weighed in a molar ratio of 1:1:1. A dispersion of 5 wt% carbon nanotubes in C<sub>2</sub>H<sub>5</sub>OH (received from Wako) was added and mixed intimately using an agate mortar and pestle. The mixture was poured into a 250 mL zirconia-lined Cr-hardened stainless steel (Cr-SS) milling pot with zirconia (YSZ) milling media (φ10 mm × 100 ZrO<sub>2</sub> balls), and 50 mL of ethanol added. Mixing was performed using

a Fritsch LP-6 at 400 rpm for 8 h with reverse rotation every 30 min. The obtained slurry was dried at 80 °C in oven. The dried powder was pulverised using an agate mortar and pestle for 1 h, after which the powder was pelletised at 50 MPa using an isostatic press machine. Using an annealing rate of 5°C/min, the pellets were fired in a horizontal quartz tubular furnace and calcined at temperatures ranging from 600 °C to 850°C for 5 h with a fixed Ar flux. The obtained pellets were thereafter transferred to the zirconia-lined Cr-hardened stainless steel milling pot with zirconia milling ball. After 24h ball-milling at 400rpm, the final MFPP/CNT composite material was prepared. The content of CNT was determined to be ~5%.

#### **Characterization of morphology, crystal structure and valence state**

The morphology of the as-prepared MFPP was characterized by using scanning electron microscopy (JEOL, JSM-890) at an acceleration voltage of 15 kV. The diffraction pattern of the as-prepared MFPP was measured on an X-ray diffractometer (RIGAKU, RINT-ULTIMA III) using Cu  $K\alpha$  radiation ( $\lambda = 1.54051\text{\AA}$ ). The diffraction patterns were recorded in the  $2\theta$  range of  $10^\circ$ – $80^\circ$  with a step size of  $0.01^\circ$ . Synchrotron X-ray diffraction (SXR) patterns of MFPP were collected at the beam line BL02B2 (SPring-8 in Japan), equipped with a large Debye-Scherrer camera. MFPP powder was filled in a glass capillary and sealed by a resin. Based on the obtained SXR patterns, the crystal structure was further refined by the Rietveld method with the program JANA2006 using the pseudo-Voigt function of Finger *et al*<sup>1, 2</sup> and drawn by the software of VESTA<sup>3</sup>. To determine the occupations of M1 and M2 sites by Fe and Mg within the lattice structure, the crystallographic information files of MFPP with different occupations were built by fixing the atomic positions and created by using VESTA. The corresponding X-ray diffraction patterns of these simulated MFPPs were predicted by

using the Reflex program implemented in the software of Materials Studio 6.1 suite.<sup>4</sup> X-ray absorption near edge spectra (XANES) measurement was employed to determine the valence state of Fe within MFPP. X-ray absorption spectra of MFPP sample and the reference compound ( $\text{FeC}_2\text{O}_4 \cdot 2\text{H}_2\text{O}$ ) were measured in the energy region of the Fe *K*-edge at room temperature in transmission mode at the beam line of the SPring-8 synchrotron radiation facility (BL14B2). The intensity of X-ray beam was measured by ionization detectors. Treatment of the raw X-ray absorption data was performed with Athena package.<sup>5</sup> Analysis of Fe *K*-edge XANES spectra was performed with the Rigaku REX 2000 program package.<sup>6</sup>

### **Electrochemical characterization**

The composite electrodes of  $\text{MgFePO}_4\text{F}$  were prepared by mixing the obtained MFPP/CNT composite with acetylene black (AB) and polytetrafluoroethylene (PTFE) in a weight ratio of 5:4:1. The electrode was then pressed and disks with a diameter of 6 mm were punched out. The punched out electrodes were pressed in between Pt meshes as the working electrode, and the typical mass loading of the active powder was *ca.* 5 mg/cm<sup>2</sup>. Thereafter, the electrode was dried *in vacuo* at 80°C. Hermetically sealed three electrode cells were assembled in an Ar-filled glove box. 0.5 M of  $\text{Mg}(\text{TFSI})_2$  in super dehydrated acetonitrile (all from Wako chemicals) was used as the electrolyte. Mg rod and Pt mesh were used as the anode (counter electrode) and the current collector, respectively. As a reference electrode, a silver wire was inserted into a solution of 0.01 M  $\text{AgNO}_3$  and 0.5 M  $\text{Mg}(\text{TFSI})_2$  in super dehydrated acetonitrile. This solution, contained in an additional glass tube, was brought into contact with  $\text{Mg}(\text{TFSI})_2$  / acetonitrile solution via a microporous glass membrane. To minimise the effect of the ohmic IR drop associated with the electrolyte resistance, the tip of

the capillary was placed as close as possible to the working electrode. Galvanostatic charge and discharge measurements in the electrolytic window range of -1.2 V to 1.5 V vs. Ag/Ag<sup>+</sup> were carried out at 25°C at a current density of C/20 and C/30. As a comparison, two-electrode cells were assembled to study the cathodic performance of MFPP in Li<sup>+</sup> electrolyte. 1 M LiClO<sub>4</sub> in mixed solvent of EC and DMC was used as electrolyte. Lithium discs were used as counter and reference electrodes. Galvanostatic charge and discharge measurements in the electrolytic window range of 1.3 V to 4.6 V vs. Li/Li<sup>+</sup> were carried out at 25°C at a current density of C/30. Prior to repeated galvanostatic measurements, MFPP was first pre-cycled to facilitate electrolyte ingress into the composite electrodes and separators. All the capacities presented in this paper were calculated based on MFPP only.

## Supplementary results

Table S1. Atomic parameters obtained from Rietveld refinement of the SXRD patterns for as-prepared MgFePO<sub>4</sub>F synthesized at 650 °C.

Atom	$g^*$	$x$	$Y$	$z$	$U^*$
Mg1	0.475	0.1831(7)	0.1683(7)	0.9636(12)	0.005
Fe1	0.525	0.1906(3)	0.2041(3)	0.9823(5)	0.005
Mg2	0.525	0.0809(7)	0.4506(10)	0.1271(13)	0.005
Fe2	0.475	0.0994(3)	0.4548(5)	0.1555(7)	0.005
P	1	0.0761(2)	0.3819(4)	0.6507(3)	0.010
O1	1	0.0567(3)	0.4734(4)	0.8297(7)	0.010
O2	1	0.9616(4)	0.2689(5)	0.6005(6)	0.010
O3	1	0.1682(5)	0.3156(6)	0.7169(5)	0.010
O4	1	0.1204(3)	0.4786(4)	0.4672(7)	0.010
F	1	0.2633(3)	0.3725(4)	0.1300(7)	0.005

\*Parameters  $g$  and  $U$  were fixed based on the parameters obtained during the preliminary refinement process.

Table S2. Atomic parameters obtained from Rietveld refinement of the SXRD patterns for as-prepared MgFePO<sub>4</sub>F synthesized at 800 °C.

Atom	$g^*$	$x$	$y$	$z$	$U^*$
Mg1	0.440	0.1794(6)	0.1663(6)	0.9551(10)	0.005
Fe1	0.560	0.1928(2)	0.2029(2)	0.9839(4)	0.005
Mg2	0.560	0.0855(7)	0.4585(9)	0.1281(11)	0.005
Fe2	0.440	0.0972(4)	0.4504(5)	0.1530(6)	0.005
P	1	0.0755(2)	0.3823(2)	0.6521(3)	0.010
O1	1	0.0558(3)	0.4761(3)	0.8274(6)	0.010
O2	1	0.9570(3)	0.2648(4)	0.6038(5)	0.010
O3	1	0.1722(4)	0.3078(4)	0.7111(4)	0.010
O4	1	0.1192(3)	0.4749(3)	0.4629(6)	0.010
F	1	0.2669(3)	0.3746(4)	0.1287(5)	0.005

\* Parameters  $g$  and  $U$  were fixed based on the parameters obtained during the preliminary refining process.

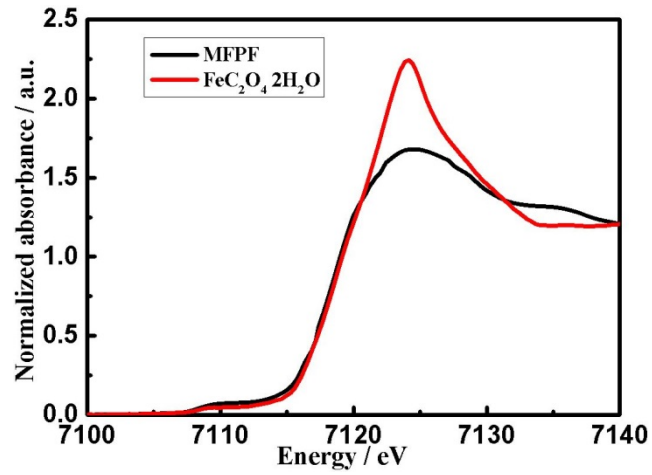


Fig. S1. Fe *K* edge X-ray absorption near edge spectra of as-prepared MFPF and  $\text{FeC}_2\text{O}_4 \cdot 2\text{H}_2\text{O}$ .

$2\text{H}_2\text{O}$  validating the octahedral coordination of  $\text{Fe}^{2+}$  in MFPF framework

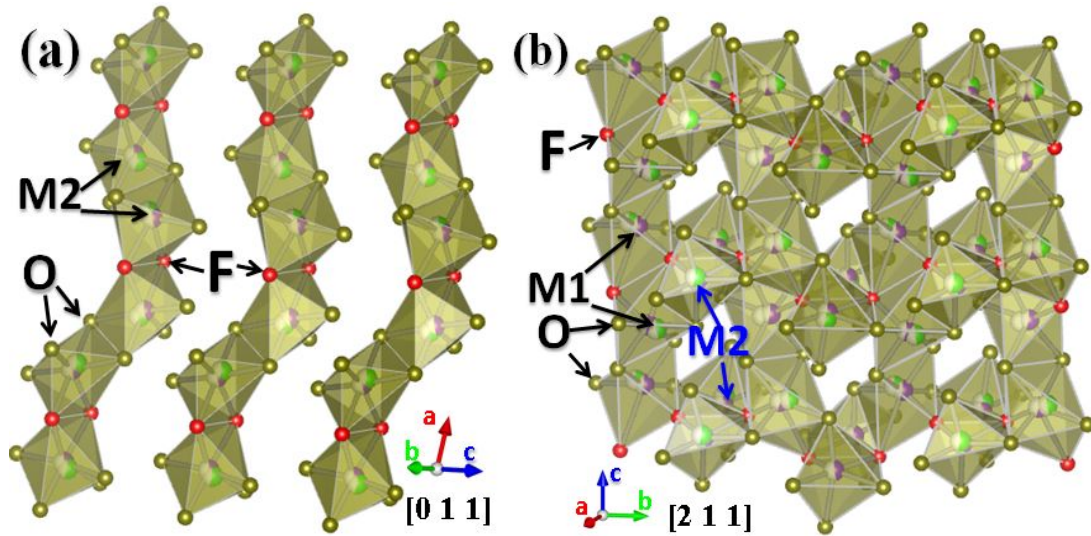


Fig. S2. 3D crystallographic representation of cationic-disordered MFPF monoclinic

framework projected along (a)  $[0\ 1\ 1]$  and (b)  $[2\ 1\ 1]$ .

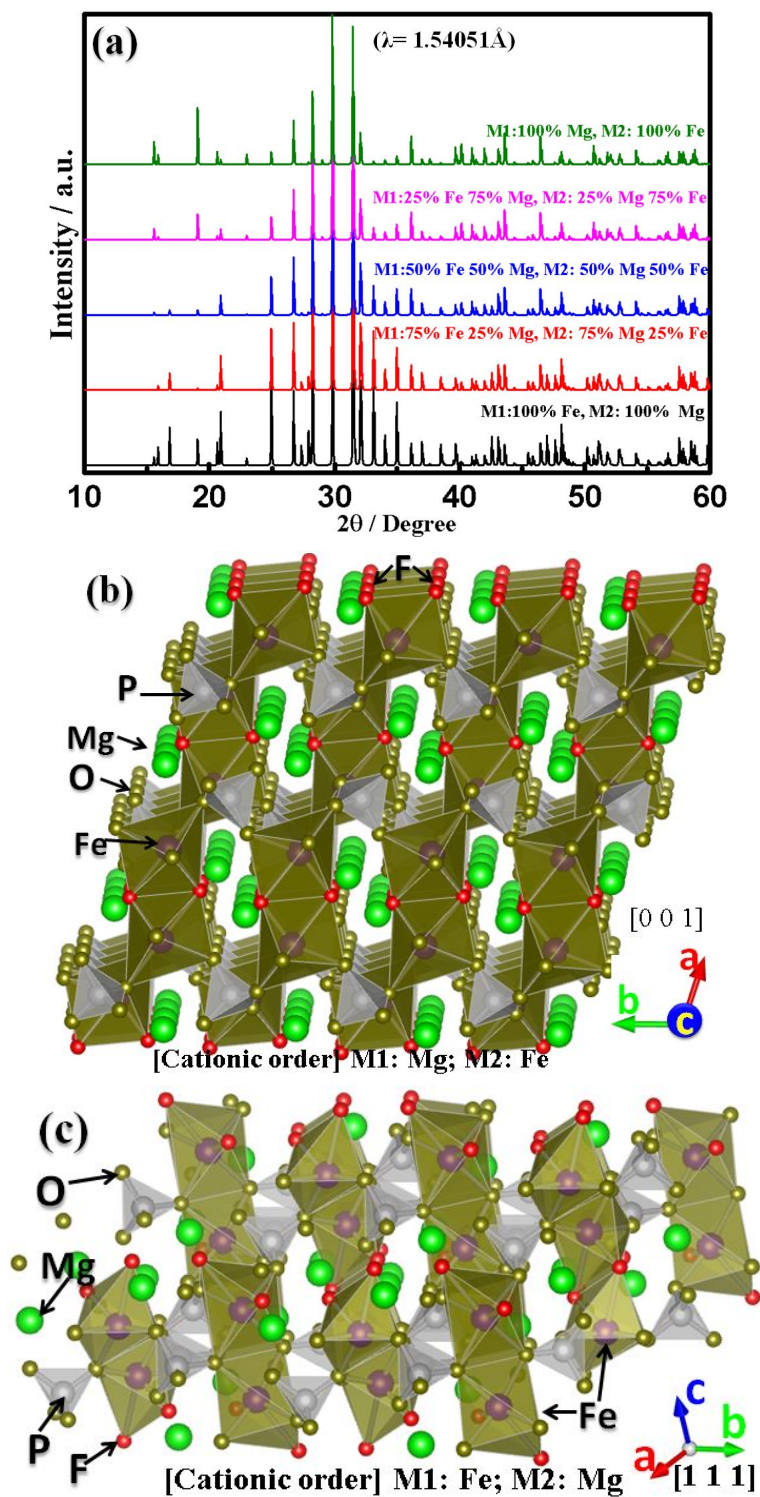


Fig. S3. (a) Simulated X-ray diffraction patterns ranging from  $10^\circ$  to  $60^\circ$  of MFPP with various occupations of Fe and Mg in M1 and M2 sites. The corresponding 3D crystallographic representations of simulated MFPP in two different cationic orderings are shown in (b) and (c).

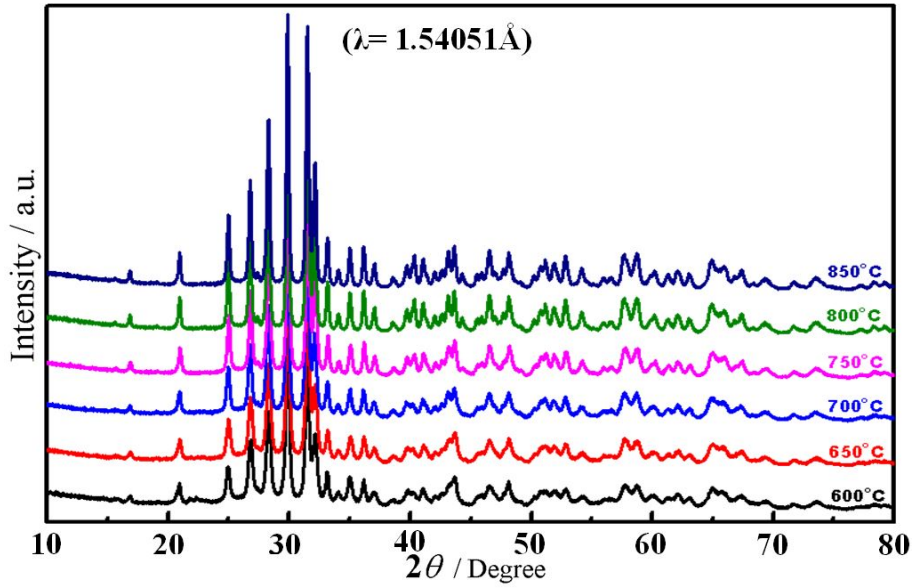


Fig. S4. X-ray diffraction patterns of  $\text{MgFePO}_4\text{F}$  prepared at different temperatures (*viz.* 600 °C, 650 °C, 700 °C, 750 °C, 800 °C and 850 °C).

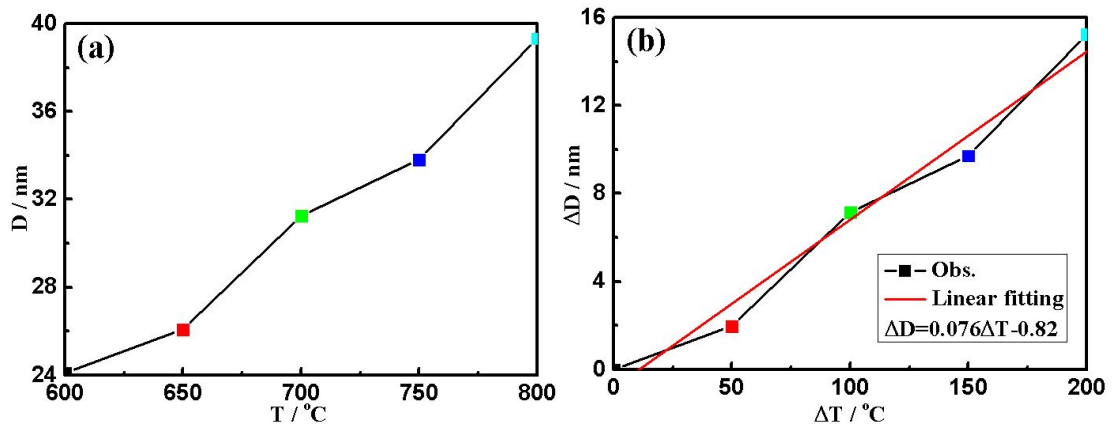


Fig. S5. (a) The crystal grain size of MFPPF sintered for 5h from 600 to 800 °C calculated by the Scherrer equation ( $D=K\lambda/\beta\cos\theta$ ).  $K$  is a dimensionless shape factor, has a typical value of about 0.9.  $\lambda$  is the X-ray wavelength, equal to 0.154 nm.  $\beta$  and  $\theta$  are the full-width at half-maximum and the Bragg angle of the diffraction peak ( $2\theta$ ) centered at  $29.8^\circ$ , respectively. (b) The linear relationship of the grain size increment vs the rising of sintering temperature.

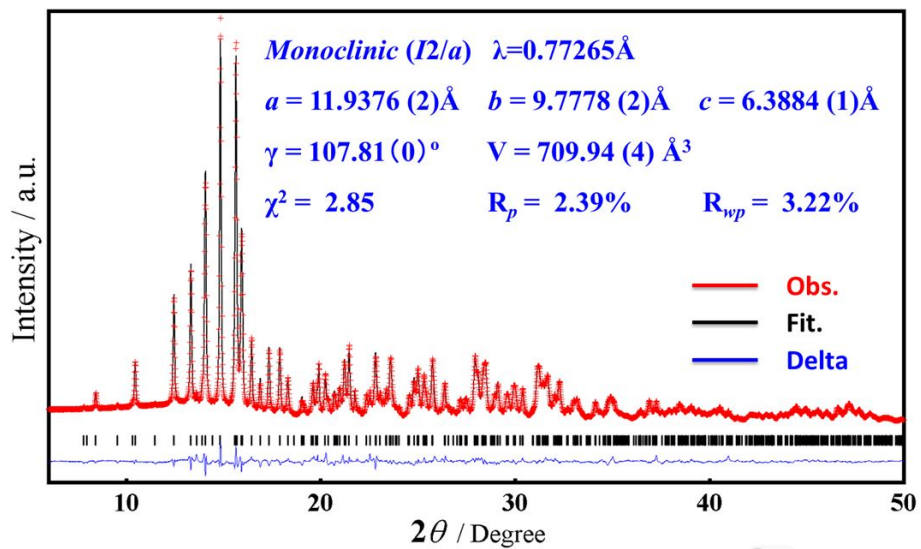


Fig. S6. Rietveld refinement result of the synchrotron XRD pattern of MFPF prepared at 800 °C.

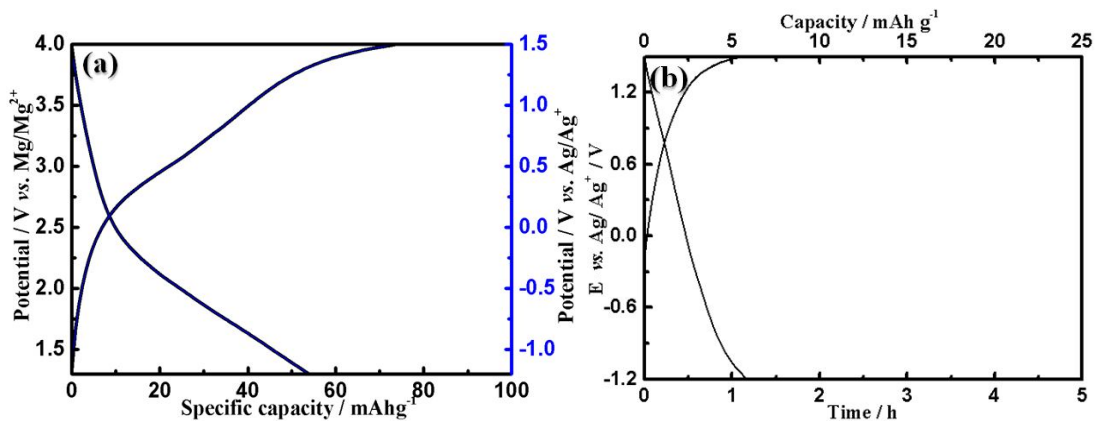


Fig. S7. Voltage (dis) charge profiles of (a) MFPP and (b) AB recorded at a current density corresponding to C/30 rate at 25°C in a Mg-ion cell

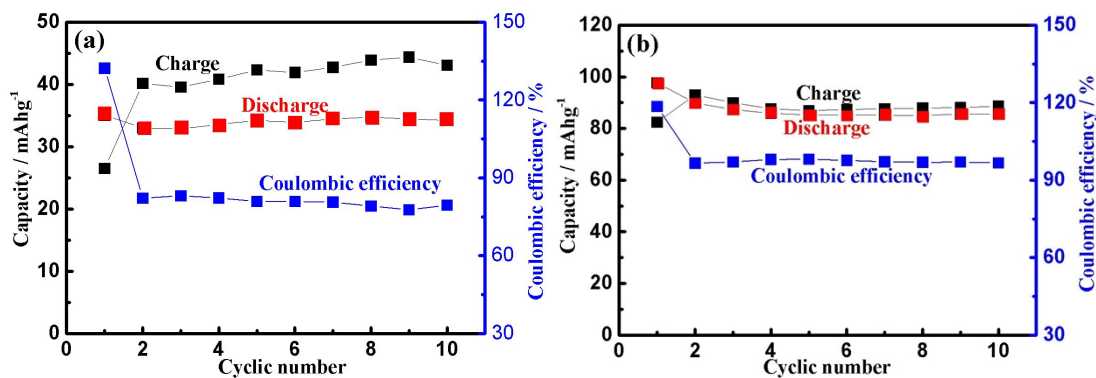


Fig. S8. Cyclic performance and coulombic efficiency of the as-prepared MFPP electrodes in a three-electrode Mg-ion cell (a) and two-electrode Li-ion cell (b).

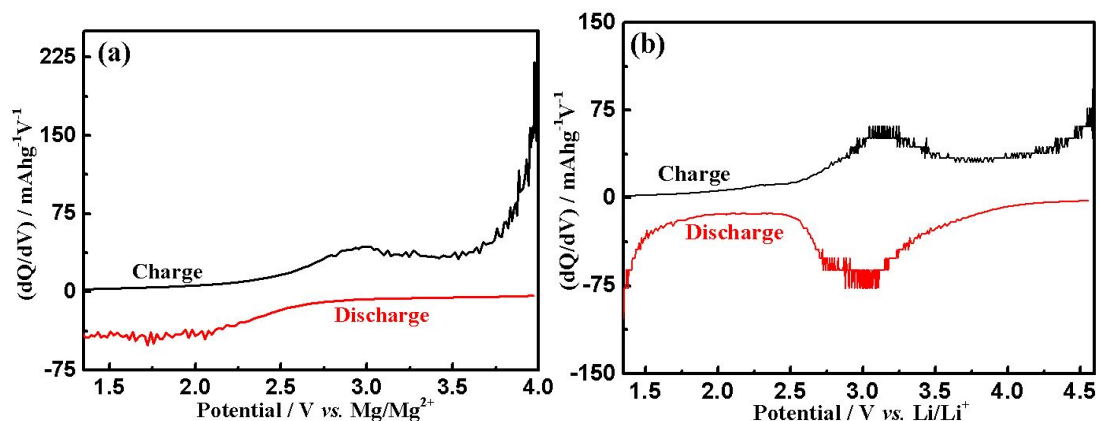


Fig. S9. Differential capacity dQ/dV plots corresponding to the tenth charge/discharge cycle of the as-prepared MFPP electrode in a three-electrode Mg-ion cell (a) and a two-electrode Li-ion cell (b).

## References

- 1 V. Petricek, M. Dusek, L. Palatinus, Jana2006-the crystallographic computing system, 2006, Praha, Czech Republic.
- 2 L.W. Finger, D. E. Cox, A. P. Jephcoat, J. Appl. Cryst., 1994, 27, 892–900.
- 3 K. Momma, F. Izumi, J. Appl. Crystallogr., 2008, 41, 653-658.
- 4 X. F. Zhou, X. Dong, Z.S. Zhao, A. R. Oganov, Y. J. Tian, and H. T. Wang, Appl. Phys. Lett., 2012, 100, 061905.
- 5 B. Ravel, M. Newville, J. Synchrotron Rad., 2005, 12, 537-541.
- 6 T. Taguchi, T. Ozawa, H. Yashiro, Phys. Scr., 2005, T115, 205-206.